

INTERDEPENDENCE BETWEEN COOLING RATE, MICROSTRUCTURE AND POROSITY IN MG ALLOY AE42

Liang Wang¹, Hongjoo Rhee¹, Sergio D. Felicelli², Adrian S. Sabau³, John T. Berry²
¹Center for Advanced Vehicular Systems, Mississippi State University, Mississippi State, MS 39762, USA
²Mechanical Engineering Department, Mississippi State University, Mississippi State, MS 39762, USA
³Metals and Ceramics Division, Oak Ridge National Laboratory, Oak Ridge, TN 37831, USA

Keywords: Magnesium alloy, AE42, Oxide film, Porosity

Abstract

Porosity is a major concern in the production of light metal parts. This work aims to identify some of the mechanisms of microporosity formation during the gravity-poured castings of magnesium alloy AE42. Two graphite plate molds and a ceramic cylindrical mold were selected to produce a wide range of cooling rates. Temperature data during cooling was acquired with type K thermocouples at 60 Hz at two or three locations of each casting. The microstructure of samples extracted from the regions of measured temperature was then characterized with optical metallography. The results of this study revealed the existence of oxide film defects, similar to those observed in aluminum alloys. The cooling rates showed significant effect on the formation of porosity.

Introduction

Magnesium cast alloys, such as AE42, are gaining increasing attention in the struggle for weight saving in the automobile industry [1]. However, in many cases the consistent production of sound AE42 castings is marred by the stubborn persistence of some defects that are difficult to remove: porosity, macrosegregation, oxide entrapment, irregularity of microstructure, etc. The formation of microporosity in particular is known to be one of the primary detrimental factors controlling fatigue lifetime and total elongation in cast light alloy components.

Many efforts have been devoted to investigate the mechanisms of porosity formation in the last 20 years. More recently, new mechanisms of pore formation based on entrapment of oxide films during the filling of aluminum alloy castings have been identified and documented [2-7]. Oxide film defects are formed when the oxidized surface of the liquid metal is folded over onto itself and entrained into the bulk liquid. A layer of air is trapped between the internal surfaces of the oxide film, which leads to the porosity formation in the solidified castings. The entrapment process due to surface turbulence is usually rapid, in the order of milliseconds, therefore the time is very limited to form new oxide film on the fresh surface, so that the entrained oxide film can be very thin, in the order of nanometers. [2]

Oxide film defects may be contained in most reactive liquid metals such as Al and Mg due to surface turbulence during the melting, pouring and transfer processes in casting. These defects have been observed on the fracture surfaces of tensile test specimens and the oxides have been identified by SEM-EDX analysis [7-8]. In contrast with the efforts devoted to Al-based cast alloys, few studies have been done in Mg alloy castings. Griffiths and Lai [8] investigated the nature of the oxide film defects in pure Mg castings. They found double oxide film defects comprised of folded MgO films on the fracture surface of tensile test bars taken from the castings.

In this study, we examined the microstructure of magnesium alloy AE42 ingots gravity-poured in plate graphite molds. Two graphite plate molds and a ceramic cylindrical mold were selected to produce a wide range of cooling rates. Temperature data during cooling was acquired with type K thermocouples at 60 Hz at two or three locations of each casting. The microstructure of samples extracted from the regions of measured temperature was then characterized with optical metallography. This work investigated the nature of oxide film and porosity defects in AE42 for different cooling rates.

Experimental Procedure

Design of casting

The cast ingots or slab castings were produced at the facilities of Oak Ridge National Laboratory (Oak Ridge, TN). Molds A and C were made of graphite. Mold type E was made of a clay-graphite material, which had a lower thermal conductivity than that of molds A and C. Molds type A and C were rectangular, while mold type E was cylindrical. The thickness of wall for molds A and C was 0.5 in (12.7 mm), while that of the E mold was 0.2 in (5.1 mm). The width, height, and thickness dimensions for molds A and C were 3×5×1.5 in (76.2×127×38.1 mm) and 5.5×11×2.25 in (140×279×57 mm), respectively. The height and outer diameter of mold E was 3.6×1.8 in (91.4×45.7 mm). The geometry of each mold is shown in Figure 1.

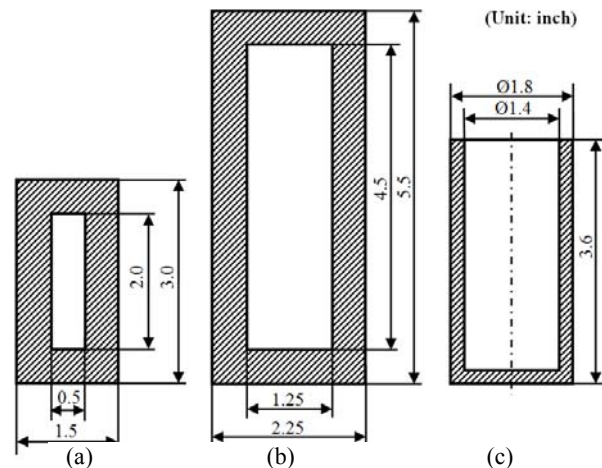


Figure 1. Cross sections of molds used for AE42 castings.
(a) Mold A: Plate graphite mold with plate thickness of 0.5 inch;
(b) Mold C: plate graphite mold with plate thickness of 1.25 inch;
(c) Mold E: cylindrical ceramic mold.

Several thermocouples were placed in the empty molds per each casting. Figure 2 shows the thermocouple fixtures on the top view of empty molds for mold type C and A in the same scale. For the C-mold, the thermocouples were placed at distances of approximately 1.35, 6.2, and 8.4 in (34.3, 157.5, and 213.4 mm) from casting end. In order to assess the reproducibility of the data, for molds A and E, two thermocouples were placed at approximately in the center of the casting, i.e., at distances of 2.3 and 1 in (58.4 and 25.4 mm), respectively, from the casting end.

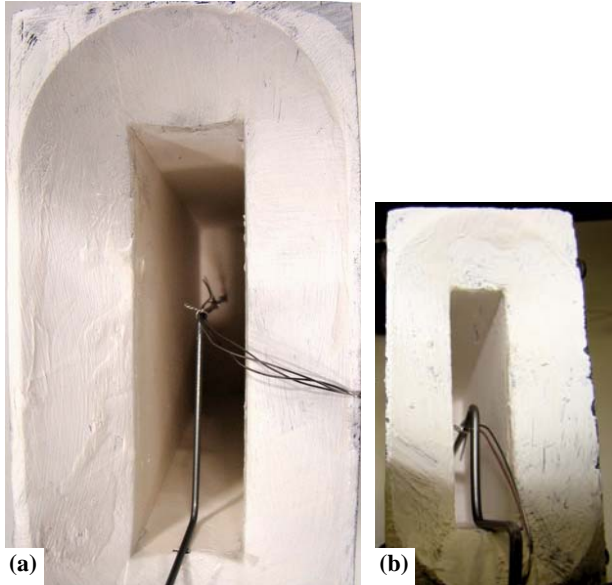


Figure 2. Top view of empty molds showing thermocouple fixtures. (a) mold type C, (b) mold type A (same scale).



Figure 3. Pouring of casting type C.

The tested AE42 alloy composition was Mg, 3.96%Al, 0.35%Mn, 0.01%Si, 0.001%Ni, 0.007%Zn, 0.0003%Fe, 0.0008%Cu, and 8ppm Be. The furnace charge was in the form of pre-alloyed ingot. The weight of the melt was 8 kg and the alloy was melted in an electrical resistance furnace. For protection, Ar and CO₂+3%SF₆ were used as cover gases. The pouring temperature

for AE42 was approximately between 680 to 700 °C. No degassing procedures were used. All castings were poured from one melt. The melt was poured directly from the crucible to minimize temperature decrease during pouring (Figure 3).

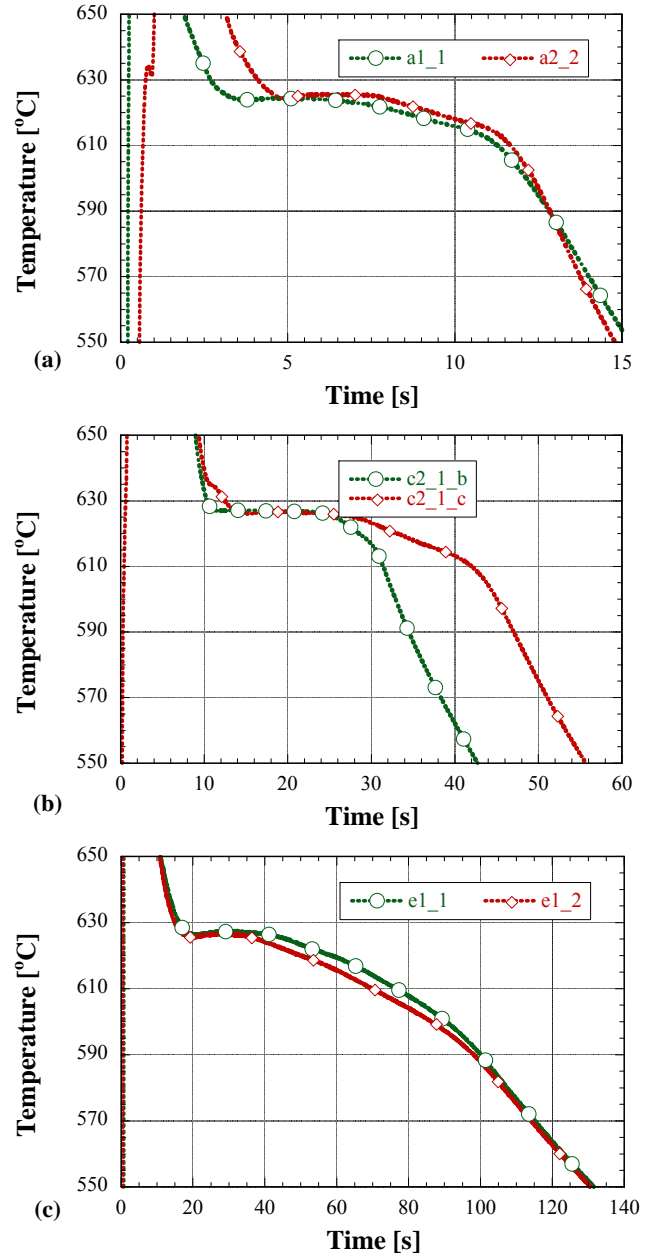


Figure 4 - Cooling curves for AE42 Mg alloy castings. (a) mold type A, (b) mold type C, (c) mold type E.

The pouring temperature was approximately 715, 695, and 725 °C for castings type C, A, and E. All the molds were not preheated and were coated with boron nitride. In order to assess the reproducibility of the results, two molds were used for each type of casting. Temperature data was acquired with thermocouples type K at approximately 60 Hz. The cooling curves are shown in Figure 4. The cooling curves are labeled in the following format:

xn_m, where x – is a letter, indicating the mold type, n – indicates casting number (1 or 2), m – indicates thermocouple (1 or 2) for molds A and E and position of thermocouples for molds type C (b-bottom of casting, c-center of casting). The cooling curves show an excellent reproducibility. The data measured by the thermocouple near the top of the casting was discarded because of turbulence in this region. As shown in Figure 4, the cooling rates for AE42 alloy castings were approximately 20, 5, and 1 °C/s for molds A, C, and E, respectively.

Sample preparation for optical metallography

Two samples for each ingot were cut near the location of the thermocouple for each as-cast ingot and then hot-mounted in phenolic resin, with one side of the plate flush with the mounted surface. The samples were then polished using a machine disc grinder. The silicon carbide abrasive papers of grade 500 and 2400 μm grits were used successively. In between papers the samples were cleaned by ethanol thoroughly. The samples were then cleaned in a sonic bath before being examined by optical microscope. Approximately 20 to 30 images were taken for each sample.

Results and Discussion

A common feature found in all the samples is that the pores were observed to be smaller at higher cooling rates. Porosity was the major defect observed in the tested specimens. Figure 5 shows typical pore morphology at a location close to the thermocouple in the AE42 C1 sample from the mold type C.

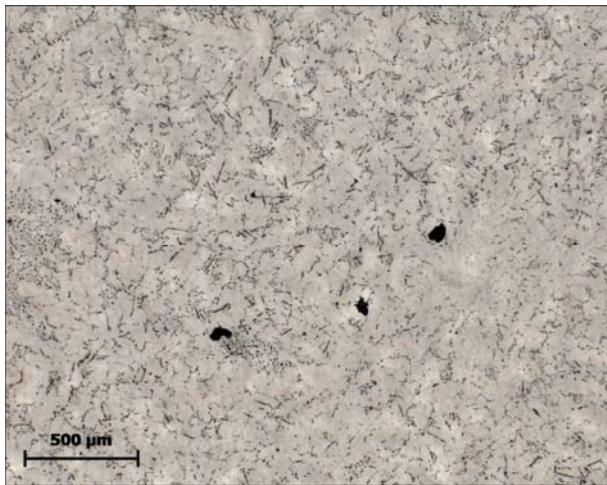


Figure 5. Typical pore morphologies formed at the location close to the thermocouple in casting AE42 C1 sample.

Figures 6-8 show the pore morphology for different samples at different cooling rates. Figure 6 shows a very clean surface for the samples A1-1 and A2-2 from the mold type A with the highest cooling rate of 20 °C/s. The maximum size of pores found in the sample is 33 μm in diameter. Figure 7 shows a group of pores found in the samples C1-1 and C2-1 from the mold type C with cooling rate of 5 °C/s. This type of pores was most probably caused by interdendritic shrinkage. Long pieces of oxide films, some longer than 1 mm, were observed in the samples E1-1 and E1-2 from the mold type E with cooling rate of 1 °C/s (Figure 8).

The distinct precipitation upon both sides of the film might suggest the former existence of a double oxide that was later torn open, with the higher precipitation occurring on the wetted side. It is interesting to note that oxide films were found only in the samples from ingots cast at the lowest cooling rate. This fact needs confirmation by examining more samples.

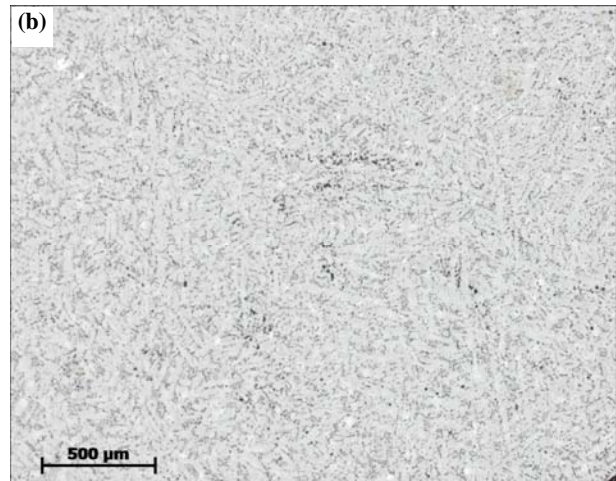
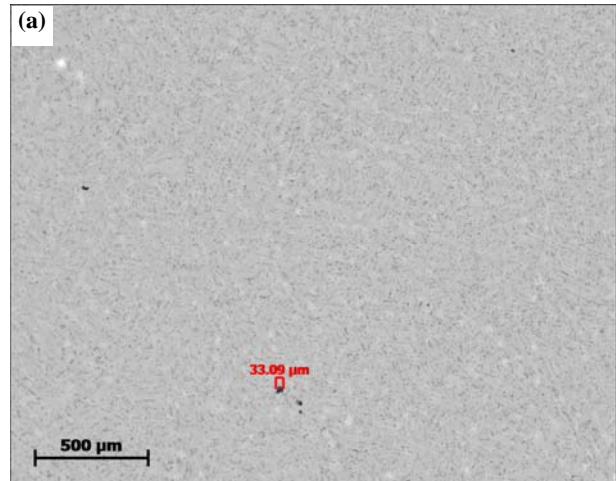
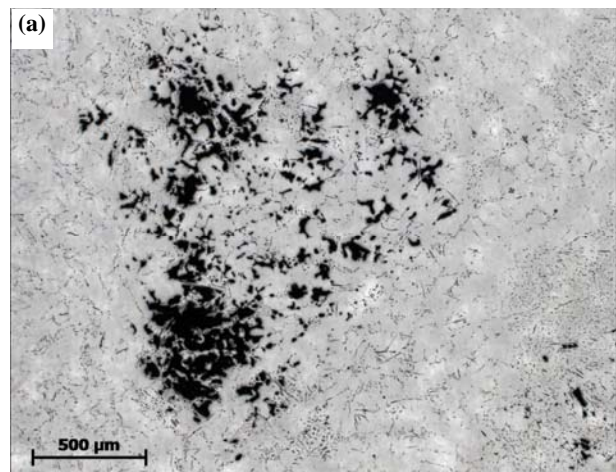


Figure 6 Typical micrographs of samples (a) A1-1, (b) A2-2.



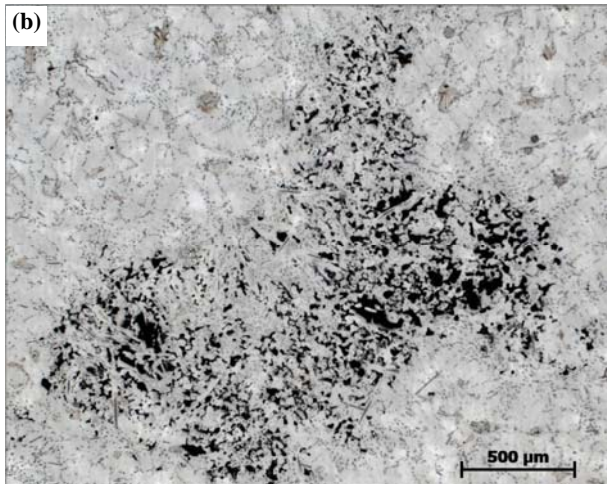


Figure 7. Typical micrographs of samples (a) C1-1, (b) C2-1, showing shrinkage porosity.

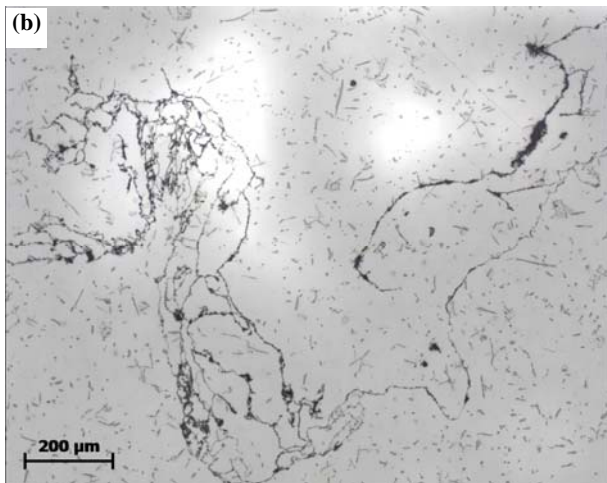
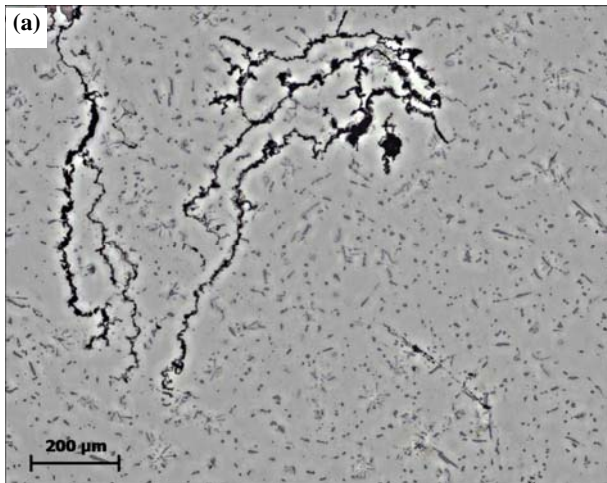


Figure 8. Typical micrographs of samples (a) E1-1, (b) E1-2, showing porosity and oxide films.

Conclusions

The microstructure of plate-shaped ingots of magnesium alloy AE42 obtained by gravity-pouring in a graphite mold was analyzed by optical metallography. Abundant porosity was found throughout the ingots. Pieces of oxide film, some of them 1 mm or longer, were also detected in many polished cross sections. Distinct features on both sides of the films suggest that they might be remnants of torn double oxide films or bifilms entrained during the pouring. The effects of cooling rate on the formation of porosity are significant. Smaller size and lower volume fraction of porosity were observed at higher cooling rate. Surprisingly, the oxide films were only found at lower cooling rates in this study. The relations between the cooling rate and oxide film are still unclear.

Acknowledgements

This work was sponsored by the National Science Foundation through grant number CTS-0553570. The authors are thankful to Prof. William Griffiths of the University of Birmingham (UK) for the helpful discussions held during his visit to MSU in Fall 2007. This work was performed in collaboration with the United States Advanced Materials Partnership (USAMP), United States Council for Automotive Research (USCAR). This research was also sponsored by the U.S. Department of Energy, Assistant Secretary for Energy Efficiency and Renewable Energy, Office of Transportation Technologies, Lightweight Vehicle Materials Program, under contract DE-AC05-00OR22725 with UT-Battelle, LLC. The authors acknowledge that this research was supported in whole by Department of Energy Cooperative Agreement No. DE-FC05-02OR22910. Such support does not constitute an endorsement by the Department of Energy of the views expressed herein. We would like to thank E.C. Hatfield and D.C. McInturff of Oak Ridge National Laboratory for assistance with casting experiments.

References

- [1] C.H. Caceres, C.J. Davidson, J.R. Griffiths, and C.L. Newton, "Effects of Solidification Rate and Ageing on the Microstructure and Mechanical Properties of AZ91 Alloy," *Materials Science and Engineering A*, 325 (2002), 344-355.
- [2] John Campbell, *Castings 2nd ed.* (Butterworth-Heinemann, London, 2003), 17-69.
- [3] X. Yang, X. Huang, X. Dai, J. Campbell, and R. J. Grant, "Quantitative Characterization of Correlations between Casting Defects and Mechanical Strength of Al-7Si-Mg Alloy Castings," *Materials Science & Technology*, 22 (2006), 561-570.
- [4] J. Campbell, "Entrapment defects," *Materials Science & Technology*, 22 (2) (2006), 127-145.
- [5] J. Knott, P.R. Beeley, J.R. Griffiths, N.R. Green, C.J. Newton, and J. Campbell, "Commentaries on 'Entrapment Defects' by J. Campbell," *Materials Science & Technology*, 22 (2006), 999-1008.
- [6] R. Raiszadeh, and W.D. Griffiths, "A Method to Study the History of a Double Oxide Film Defect in Liquid Aluminum Alloys," *Metallurgical and Materials Transactions. B*, 37 (2006), 865-871.
- [7] J. Mi, R.A. Harding, M. Wickins, and J. Campbell, "Entrapped Oxide Films in TiAl Castings," *Intermetallics*, 11 (2003), 377-385.

- [8] W.D. Griffiths, and N.W. Lai, "Double Oxide Film Defects in Cast Magnesium Alloy," *Metallurgical and materials transactions A*, 38 (2007), 190-196.
- [9] W.D. Griffiths, "An SEM Study of High Pressure Die Cast Mg Alloy Castings" (Report #MSU.CAVS.CMD.2008-R0023, Center for Advanced Vehicular Systems, Mississippi State University, 2007)